Proceedings of 20th International Congress on Acoustics, ICA 2010

23-27 August 2010, Sydney, Australia

Computing diffraction integrals with the numerical method of steepest descent

U. Peter Svensson (1), Andreas Asheim (2)

(1) Dept. of Electronics and Telecommunications, Norwegian University of Science and Technology, Trondhiem, Norway
(2) Dept. of Mathematics, Norwegian University of Science and Technology, Trondhiem, Norway

PACS: 43.20.El

ABSTRACT

A common type of integral to solve numerically in computational room acoustics and other applications is the diffraction integral. Various formulations are encountered but they are usually of the Fourier-type, which means an oscillating integrand which becomes increasingly expensive to compute for increasing frequencies. Classical asympotic solution methods, such as the stationary-phase method, might have limited accuracy across the relevant frequency range. The method of steepest descent is known to offer efficient evaluation of such integrals but for most diffraction integrals, the optimum deformed integration path might be impossible to find analytically. A recent numerical version of the method of steepest descent finds an approximate path numerically and this paper will show the application of this method to one specific edge diffraction integral which is valid for finite and infinite edges. The required integration path sections are found numerically via applying a Taylor expansion of the integrand oscillator function, involving up to the fourth-order derivative for this example, and a subsequent series inversion. Once the path is avaliable, two efficient quadrature methods are used for the exponentially decaying integrands, Gauss-Laguerre and Gauss-Hermite. The method is compared with brute-force numerical integration using Gauss-Kronrod quadrature in the Matlab implementation. Numercial examples demonstrate that the new method has a computation time which is independent of frequency and of edge length, whereas that of the brute-force method depends heavily on frequency as well as edge length. It is shown that the accuracy of the new method decreases for low frequencies and for geometrical cases where the receiver point is near a zone boundary. Methods to tackle these limitations are outlined.

INTRODUCTION

Edge diffraction modeling is used in studies of, e.g., noise barriers [1], loudspeaker enclosures [2], room acoustics [3], sea floor scattering [4] as well as other scattering cases. The term edge diffraction refers to the component of the sound field which complements the spatially discontinuous geometrical solutions so that the total sound field is correct and therefore continuous in space [5]. Classical solutions have been presented by Kirchhoff for the diffraction of a thin half-plane which is hit by a plane wave [6], and by Macdonald in 1915 for the diffraction from a rigid wedge which is insonified by a point source [7].

In 1957, Biot and Tolstoy presented an explicit time-domain expression for the diffraction from a rigid wedge as caused by a point source. This solution was later explored by Medwin who suggested a decomposition into contributions by secondary sources along the edge, which could then even by expanded to second-order diffraction [1,8]. Medwin's decomposition into secondary edge source contributions was later put in a form with analytic directivity functions by Svensson et al [9, 10]. This analytic directivity function form was finally presented in a frequency-domain form [11] which was shown to be identical to classical contour integral solutions [5, 12]. The equivalence between those classical contour integral solutions and the time-domain solution by Biot and Tolstoy has also been demonstrated by Chu [13].

Another family of high-frequency asymptotic solutions stem from the geometrical theory of diffraction [14] and the uniform asymptotical theory of diffraction [15]. One asymptotic solution was transformed into a time-domain solution by Vanderkooy [2]. Yet another family of solutions is based on the Kirchhoff diffraction approximation [16,17] which has been shown to not be asymptotically correct for high frequencies in some cases [18].

A unique feature of the methods presented in [1,9-11] is that they can be applied to finite edges. Obviously, finite edges require higher-order diffraction, and the methods suggested for higher orders have so far not included so-called slope diffraction [19-20].

Common to all these formulations is that they must be computed numerically. For time-domain formulations, such computations require for each edge a large number of very-short-range integrals with a well-behaved, non-oscillatory, real-valued integral [10, 21]. In the frequency domain, a single edge is described by a single long-range integral of an oscillatory, complex-valued integral, which becomes increasingly expensive as the frequency increases. The topic of this paper is how to compute such oscillatory diffraction integrals.

The classical problem of numerical integration of oscillatory integrals can be solved with asymptotic methods such as the method of stationary phase or the saddle point method [22-

23] but they get increasingly inaccurate at lower frequencies. The method of steepest descent [23] is very efficient and accurate but requires the access to the path of steepest descent after applying analytic continuation of the integrand. Such paths can typically not be found for anything but very simple integrands, and for the diffraction integrals studied here, such paths can not be found analytically. However, recent developments have lead to the numerical method of steepest descent [24-25] which uses an approximation of these paths [26] and the result is a very efficient method as will be shown in this paper. A more detailed presentation can be found in [27].

In the theory chapter, the specific diffraction integral to be solved is presented, and brief descriptions of the classical method of steepest descent as well as the numerical method of steepest descent are given. In a chapter of numerical examples the accuracy and computation time for the new method, as well as benchmark methods, are given. Limitations and further developments are discussed in chapter X and conclusions are drawn in chapter Y.

The edge diffration integral

The integrals of interest here are Fourier-type integrals, that is, integrals that can be written on the form

$$I = \int_a^b f(z) e^{jkg(z)} \, \mathrm{d}z, \tag{1}$$

where the function $g(z)$ is called the oscillator function. Integrals of this type are increasingly expensive to compute numerically as the wave number k, or frequency, increases. Here, the focus is on one particular integral, which gives the diffracted wave from a single finite or infinite edge [Svensson 2009],

$$I = -\frac{\nu}{4\pi} \sum_{i=1}^{4} \int_a^b \frac{\beta_i}{m \cdot l} e^{-jk(m+l)} \, \mathrm{d}z, \tag{2}$$

where β, m, and l are all real-valued functions of z. Writing this integral on the form in Eq. (1), the oscillator function g is then,

$$g(z) = -m - l = -\sqrt{(z - z_S)^2 + r_S^2} - \sqrt{(z - z_R)^2 + r_R^2} \tag{3}$$

where z_S, r_S, z_R, r_R are geometrical parameters as illustrated in Figure 1. The functions m and l are also geometrical entities as shown in Figure 1, and the functions β_i are

$$\beta_i = \frac{\sin(\nu\varphi_i)}{\cosh(\nu\eta) - \cos(\nu\varphi_i)} \tag{4}$$

where the angles φ_i are

$$\varphi_1 = \pi + \theta_S + \theta_R, \quad \varphi_2 = \pi + \theta_S - \theta_R$$
$$\varphi_3 = \pi - \theta_S + \theta_R, \quad \varphi_4 = \pi - \theta_S - \theta_R \tag{5}$$

and η is an auxiliary function

$$\eta = \cosh^{-1} \frac{(z - z_S)(z - z_R) + ml}{r_S r_R}. \tag{6}$$

The angles θ_S and θ_R are shown in Figure 1.

The method of steepest descent

For Fourier integrals, on the form in Eq. (1), where the f and g functions can be assumed to be analytic functions, Cauchy's integral theorem implies that the integration path can be deformed into the complex plane without changing the

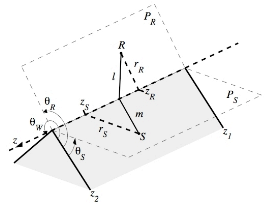

Figure 1. Illustration of the wedge and the relevant geometrical parameters.

integral's value. Then, a path can be chosen such that the oscillations of the integrand are removed. This will be fulfilled if the deformed path is such that the real part of $g(z)$ is kept constant. Figure 2 illustrates a deformed path from integration range endpoint a to the other endpoint b, for the oscillator function in Eq. (3). A geometry example was chosen with $r_S = 1$ m, $z_S = -1$ m, $r_R = 1.5$ m, $z_R = 0.75$ m. The edge extends from $a = -2$ m to $b = 2$ m.

If there happen to be stationary-phase points along the original integration range, i.e., points where $g'(z) = 0$, then crossing deformed paths, as also indicated in Figure 2, must be constructed. For all these deformed path sections the oscillator function are on the form

$$g(z) = \xi + jp = g(z_{ep/sp}) + jp = g[h_z(p)] \tag{7}$$

where ξ is a constant, which must then be given by the oscillator function's value at either one of the endpoints of the original integration range, z_{ep}, or at a stationary point, z_{sp}, where the deformed path section crosses the original integration range. The imaginary part of the function $g(z)$ along the deformed path section is described by a parameter p. With these deformed paths described by the function $h_z(p)$, the integral will be given by a sum of contributions. These contributions have one of two forms, the first one of which is valid for the two paths that connect to the integration range endpoints, z_{ep},

$$I = e^{jkg(z_{ep})} \int_0^\infty f[h_z(p)] h_z'(p) e^{-kp} \, \mathrm{d}p. \tag{8}$$

The second form applies to paths that connect to stationary points, z_{sp},

$$I = 2e^{jkg(z_{sp})} \int_{-\infty}^\infty f[h_z(p^2)] h_z'(p^2) p e^{-kp^2} \, \mathrm{d}p. \tag{9}$$

It should be noted that in Eq. (9), the two paths that cross the original integration range on the real axis through a stationary point, as seen in Figure 2, have been combined into a single integral. An integral on the form in Eqs. (8) or (9) will then have no oscillation factor in the integrand but rather an exponentially decaying factor, e^{-kp} or e^{-kp^2}, which dies out faster the higher the wavenumber k is. Such numerical integration can be solved efficiently with Gaussian quadrature as shown below. A problem is, however, that finding the path $h_z(p)$, which fulfills Eq. (7), on an analytical form is not possible, if the oscillator function is even moderately complex. Therefore, a Taylor series expansion of the path can be employed, that is, to write the path on the form

$$h_z(p) \approx z_{ep} + \sum_{i=1}^{m} a_i p^i. \tag{10}$$

The (complex) coefficients a_i can be found via a Taylor expansion of the oscillator function in Eq. (3). For a stationary point, a slightly different form is used for the path,

$$h_z(p) \approx z_{sp} + \sum_{i=1}^{m} a_i \sqrt{|p|}^{\,i}. \tag{11}$$

The m-th coefficient will involve derivatives of g of the m-th order, and the first few coefficients are

$$a_1 = \frac{j}{g'(z_{ep})},$$

$$a_2 = \frac{1}{2} \frac{g''(z_{ep})}{[g'(z_{ep})]^3},$$

$$a_3 = -\frac{a_1}{6} \frac{g'(z_{ep}) g^{(3)}(z_{ep}) - 3[g''(z_{ep})]^2}{[g'(z_{ep})]^4},$$

for integration range endpoints z_{ep}, and

$$a_1 = s\sqrt{\frac{2j}{g''(z_{sp})}},$$

$$a_2 = -\frac{j}{3} \frac{g^{(3)}(z_{sp})}{[g''(z_{sp})]^2},$$

$$a_3 = \frac{ja_1}{36} \frac{[5g^{(3)}(z_{sp})]^2 - 3g''(z_{sp}) g^{(4)}(z_{sp})}{[g''(z_{sp})]^3},$$

for stationary points z_{sp}. In the expression for a_1, the parameter $s = \mathrm{sign}(p\, g''(z_{sp}))$, which leads to that $p < 0$ corresponds to the incoming path (towards the stationary point) and $p > 0$ corresponds to the outgoing path. The derivatives of the oscialltor function $g(z)$ on the form in Eq. (3) are straightforward to derive.

These Taylor series expansions certainly have limited accuracy as the path diverges from the real axis, as indicated in Fig. 2. However, the exponentially decaying factor in the integral which is to be solved, makes sure the integral can be solved accurately with Gaussian quadrature as shown in the next subsection.

The numerical method of steepest descent

Once the paths. $h_z(p)$ are available, then there are two types of integrals to solve, as given by Eqs. (8) and (9). For the path sections to and from integration range endpoints, z_{ep}, the integral to solve is the one in Eq. (8). This is a form for which Gauss-Laguerre quadrature can be used, leading to

$$I \approx \frac{1}{k} e^{jkg(z_{ep})} \sum_{i=1}^{n} w_i f[h_z(x_i/k)] h_z'(x_i/k). \tag{12}$$

For the stationary point, the integral has a slightly different form, see Eq. (9), and Gauss-Hermite quadrature can be employed instead, which yields

$$I \approx \frac{2}{k} e^{jkg(z_{sp})} \sum_{i=1}^{n} w_i f[h_z(x_i^2/k)] h_z'(x_i^2/k). \tag{13}$$

The weighting factors, w_i, and evaluation points, x_i, for the Gauss-Laguerre case are given in Table 1. It can be noted that

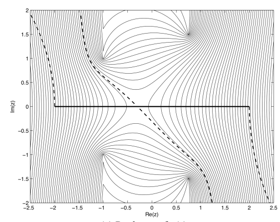

(a) Real part of $g(z)$

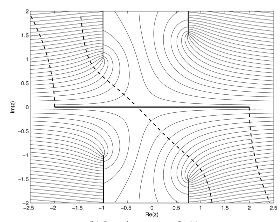

(b) Imaginary part of $g(z)$

Figure 2. Example of the oscillator function $g(z)$ in Eq. (3) Dashed lines illustrate approximate paths of steepest descent. (a) The real part of $g(z)$, and the finite edge is illustrated with a thick line. (b) The imaginary part of $g(z)$. Thick lines indicate the edge, and branch cuts for Im $[g(z)]$.

the whole set of values (for $i = 1,\ldots,n$) will depend on the truncation value n. Further coefficients can be derived as described in [28].

Table 1. Sets of evaluation points, x_i, and weighting factors, w_i, for the Gauss-Laguerre quadrature.

	x_i	w_i
$n = 1$	1	1
$n = 2$	0.585786	0.853553
	3.414213	0.146447
$n = 3$	0.415775	0.711093
	2.294280	0.278518
	6.289945	0.0103893

Table 2. Sets of evaluation points, x_i, and weighting factors, w_i, for the Gauss-Hermite quadrature.

	x_i	w_i
$n = 1$	0	1
$n = 2$	±0.707107	0.886227
$n = 3$	0	1.18164
	±1.22474	0.295409

Some numerical issues

In general, there might be any number of stationary points along the integration range but for the oscillator function in Eq. (3), a single stationary point exists, and it is the so-called apex point, z_{apex}. This is the point on the edge through which the shortest path from the source, via the edge to the receiver passes, and it is given by

$$z_{apex} = \frac{z_R r_S + z_S r_R}{r_S + r_R}. \tag{14}$$

Furthermore, a stationary point can be of first or higher order, corresponding to which is the first derivative thatis non-zero. For the integral studied here, the (single) stationary point is of order 1, meaning that $g'(z_{apex}) = 0$, while $g''(z_{apex}) \neq 0$. Stationary points of order n would have n+1 branches of the solution to Eq. (7).

The oscillator function $g(z)$ might have branch cuts, and the one studied here, in Eq. (3), does indeed have such cuts. They are illustrated in Fig. 2 (b), where the imaginary part of $g(z)$ display discontinuities at the four cuts which appear as lines perpendicular to the real axis, and starting at the four points

$$z = z_S \pm jr_S \text{ and } z = z_R \pm jr_R. \tag{15}$$

An important observation is that those branch cuts are steepest descent paths, and they don't connect to the real axis, which means that the steepest descent paths that start/end at the real axis will (analytically) never cross those branch cuts. For, approximated paths, however, there is the potential risk that there could be a crossing of the branch cuts. It can be shown that for a two-term approximation of the path, the following geometrical criterion must be fulfilled in order to avoid any such branch cut crossings [27],

$$\frac{|z_S - z_R|}{r_S + r_R} < 1. \tag{16}$$

A final issue to address is that the non-oscillator part of the integrand in Eq. (3), that is, $f(z)$ in Eq. (2), has singularities when the receiver passes a zone boundary, where either the direct sound or the specular reflection suddenly appears/disappears. This singularity causes problem for the method presented here, as will be demonstrated in the numerical examples below. Two approaches are possible in order to solve this problem. A simple approach is to use an analytical approximation for the integrand in a small interval around the apex point, since the singularity is local around there. Such an approach was described in [21] for a time-domain formulation of the integral in Eq. (2), and has also been tested for the present method in [27]. A more advanced approach would be to apply generalized Gaussian quadrature, as outlined in [29].

NUMERICAL EXAMPLES

A few numerical examples are presented below. One finite wedge has been chosen as a demonstration case, with the geometrical parameters $r_S = 2$ m, $\theta_S = \pi/4$, $z_S = 0$ m, $r_R = 5$ m, $\theta_R = 3\pi/2$, $z_R = 0$ m, $\theta_W = 3\pi/2$, and with the wedge extending from -5 m to 5 m. As a benchmark solution, the application of Gauss-Kronrod quadrature, as implemented in the Matlab function *quadgk*, is used. A very small tolerance value (2e-14) is set for this benchmark numerical integration. Furthermore, for one case, the impulse response was calculated as in [10,21] and after applying an FFT, results could be compared with the new method and the benchmark method. A sampling frequency of 48 kHz was used for this time-domain calculation. The new method has been implemented in Matlab, and while Matlab implementations do not directly give the most efficient implentations, a comparison between methods should still be valid.

Effect of frequency on accuracy and computation time

The effect of frequency on the accuracy of the new method is illustrated in Figure 3, together with one example of an impulse response based calculation using a sampling frequency of 48 kHz. First, it can be observed that with the new method, a machine precision level of the errors is achieved for higher frequencies, but the error is clearly limited at lower frequencies. Still, a relative error below 1e-3, clearly acceptable in many circumstances, results from 50 Hz and up for the chosen geometry, as long as 20 quadrature points are used. Interestingly, the impulse response based result is quite accurate at low frequencies but the error increases with frequency so the performance is quite mediocre for higher frequencies. The number of Gaussian quadrature points has a large effect on the accuracy, but quite a limited effect on the computation time. Table 1 presents computation time results for a few frequencies, and as expected, the benchmark method gets more and more demanding, computation-wise, as the frequency increases. All these timing experiments were run using Matlab on a high-end Dell workstation.

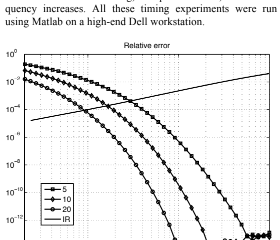

Figure 3. Relative error as function of frequency for the new method, with different number of quadrature points. Also presented as 'IR' is the result from an impulse response-based calculation.

Table 3. Timing examples

Frequency	Benchmark method	New method
0.5 kHz	5.7 ms	1-2 ms
1 kHz	6.5 ms	1-2 ms
10 kHz	19.1 ms	1-2 ms
20 kHz	29.6 ms	1-2 ms

Breakdown near zone boundaries

As a test of the new method's performance near zone boundaries, the same geometry was studied but here the receiver angle was varied along an arc such that $\theta_R \in [0, 3\pi/2]$. Thereby, the receiver will cross the two zone boundaries, one at $\theta_R = 3\pi/4 \approx 2.36$ and one at $\theta_R = 5\pi/4 \approx 3.93$. As before, benchmark results were computed using quadgk and a very low tolerance value. Figure 3 shows the relative error for the new method as function of receiver angle, and for two frequencies, 1 kHz and 10 kHz. As can be seen in the figure, large errors result around the two zone boundaries. Furthermore, the region of inaccurate results is larger for the lower frequency. The number of quadrature points has a strong influence on the relative error near the boundaries. As discussed above and in [21], the singularity issues occur for a very small range of the integration range and consequently, that small range could be treated separately, either using another quadrature method or by using an analytical approximation as in [21]. Yet another possibility to tackle the problems in the areas around the zone boundaries is to apply generalized Gaussian quadrature, as in [29], for this specific integral.

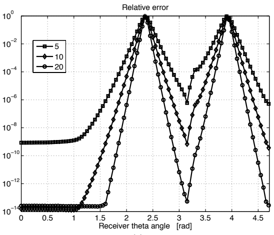

(a)

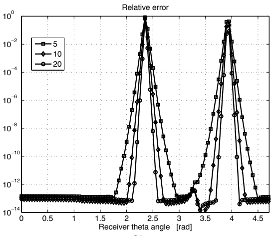

(b)

Figure 4. Relative error as function of receiver angle θ_R for (a) 1 kHz and (b) 10 kHz.

CONCLUSIONS

The high accuracy and efficiency of a new numerical method for solving diffraction integrals has been demonstrated. Special care needs to be taken for receiver positions that are close to the zone boundaries, but ways to do this have been outlined. The accuracy decreases for low frequencies, but on the other hand, classical quadrature methods are very efficient for lower frequencies. This new method would be equally applicable to other Fourier-type integrals as well.

REFERENCES

1 H. Medwin, "Shadowing by finite noise barriers" *J. Acoust. Soc. Am.* **69**, 1060–1064 (1981)
2 J. Vanderkooy, "A simple theory of cabinet edge diffraction" *J. Aud. Eng. Soc.* **39**, 923–933 (1991)
3 R. R. Torres, U. P. Svensson, and M. Kleiner, "Computation of edge diffraction for more accurate room acoustics auralization" *J. Acoust. Soc. Am.* **109**, 600–610 (2001)
4 R. S. Keiffer and J. C. Novarini, "A time domain rough surface scattering model based on wedge diffraction: Application to low-frequency backscattering from two-dimensional sea surfaces" *J. Acoust. Soc. Am.* **107**, 27–39 (2000)
5 A. D. Pierce, *Acoustics* (McGraw-Hill, New York, 1981)
6 A. Sommerfeld, "Mathematische Theorie der Diffraction" *Math. Ann.* **47**, 317-374 (1896)
7 T. M. Macdonald, "A class of diffraction problems" *Proc. Lond. Math. Soc.* **14**, 410–427 (1915)
8 M. A. Biot and I. Tolstoy, "Formulation of wave propagation in infinite media by normal coordinates with an application to diffraction" *J. Acoust. Soc. Am.* **29**, 381–391 (1957)
9 H. Medwin, E. Childs, and G. M. Jebsen, "Impulse studies of double diffraction: A discrete Huygens interpretation" *J. Acoust. Soc. Am.* **72**, 1005–1013 (1982)
10 U. P. Svensson, R. I. Fred, and J. Vanderkooy, "An analytic secondary source model of edge diffraction impulse responses" *J. Acoust. Soc. Am.* **106**, 2331–2344 (1999)
11 U. P. Svensson, P. T. Calamia and S. Nakanishi, "Frequency-domain edge diffraction for finite and infinite edges" *Acta Acustica/Acustica* **95**, 568–572 (2009)
12 J. Bowman and T. Senior, "The wedge" in *Electromagnetic and acoustic scattering by simple shapes* ed. J. Bowman, T. Senior, and P. Uslenghi, (Hemisphere Publishing Corporation, New York, 1969), chapter 6
13 D. Chu, T. K. Stanton, and A. D. Pierce, "Higher-order acoustic diffraction by edges of finite thickness" *J. Acoust. Soc. Am.* **122**, 3177–3194 (2007)
14 J. B. Keller, "Geometrical theory of diffraction" *J. Opt. Soc. Am.* **52**, 116-130 (1962)
15 R. G. Kouyoumjian and P. H. Pathak, "A uniform geometrical theory of diffraction for an edge in a perfectly conducting surface" *Proc. IEEE* **62**, 1448–1461 (1974)
16 T. F. W. Embleton, "Line integral theory of barrier attenua- tion in the presence of the ground" *J. Acoust. Soc. Am.* **67**, 42-45 (1980)
17 Y. Sakurai and K. Nagata, "Sound reflections of a rigid plane and of the "live end" composed by those panels" *J. Acoust. Soc. Jpn.* **2**, 5-14 (1981)
18 G. M. Jebsen and H. Medwin, "On the failure of the Kirchhoff assump- tion in backscatter" *J. Acoust. Soc. Am.* **72**, 1607-11 (1982)
19 J. E. Summers, *Reverberant acoustic energy in auditoria that comprise systems of coupled rooms*, Ph.D. dissertation, Rensselaer Polytechnic Institute, Troy, NY, USA (2003)
20 P. T. Calamia, *Advances in Edge-Diffraction Modeling for Virtual-Acoustic Simulations*, Ph.D. dissertation, Dept. of Computer Science, Princeton University, Princeton, N. J., USA (2009)
21 U. P. Svensson and P. T. Calamia, "Edge-diffraction impulse responses near specular-zone and shadow-zone boundaries" *Acta Acustica united with Acustica* **92** 501-512 (2006)
22 F. W. J. Olver, *Asymptotics and Special Functions* (Academic Press, New York, 1974)
23 R. Wong, *Asymptotic approximations of integrals* (SIAM Classics, Philadelphia, 2001)

24 D. Huybrechs and S. Vandewalle, "On the evaluation of highly oscillatory integrals by analytic continuation" *SIAM J. Numer. Anal.* **44**, 1026–1048 (2006)
25 D. Huybrechs and A. Deano, "Complex Gaussian quadrature of oscillatory integrals" *Numerische Mathematik*, **112**, 197–219 (2009)
26 A. Asheim and D. Huybrechs, "Asymptotic Analysis of Numerical Steepest Descent with Path Approximations" *Found. Comp. Math.,* doi 10.1007/s10208-010-9068-y (2010)
27 A. Asheim and U. P. Svensson, "Efficient evaluation of edge diffraction integrals using the numerical method of steepest descent," provisionally accepted for publication in *J. Acoust. Soc. Am.*, (2010)
28 G. H. Golub and J. H. Welsch, "Calculation of Gauss Quadrature Rules," *Mathematics of Computation* **23**, 221–230+s1–s10, (1969)
29 D. Huybrechs and R. Cools, "On generalized Gaussian quadrature for singular and nearly singular integrals" Report TW-523 (Dept. of Computer Science, K. U. Leuven, Leuven, Belgium, 2008)